



HAL
open science

A study of vTEC above Nepal exploring different calibration techniques, including a comparison with the NeQuick-2 model

P. Poudel, A. Silwal, B D Ghimire, S P Gautam, M. Karki, N P Chapagain,
B. Adhikari, D. Pandit, C. Amory-Mazaudier

► To cite this version:

P. Poudel, A. Silwal, B D Ghimire, S P Gautam, M. Karki, et al.. A study of vTEC above Nepal exploring different calibration techniques, including a comparison with the NeQuick-2 model. *Astrophysics and Space Science*, 2022, 367 (4), pp.41. 10.1007/s10509-022-04041-w . hal-03708453

HAL Id: hal-03708453

<https://hal.science/hal-03708453>

Submitted on 29 Jun 2022

HAL is a multi-disciplinary open access archive for the deposit and dissemination of scientific research documents, whether they are published or not. The documents may come from teaching and research institutions in France or abroad, or from public or private research centers.

L'archive ouverte pluridisciplinaire **HAL**, est destinée au dépôt et à la diffusion de documents scientifiques de niveau recherche, publiés ou non, émanant des établissements d'enseignement et de recherche français ou étrangers, des laboratoires publics ou privés.

Study of VTEC above Nepal with different calibration techniques, and comparison with NeQuick 2 model

P. Poudel¹, A. Silwal¹, B. D. Ghimire^{2,*}, S. P. Gautam³, M. Karki⁴, N. P. Chapagain⁴, B. Adhikari², D. Pandit², C. Amory-Mazaudier^{5,6}

¹Patan Multiple Campus, Tribhuvan University, Lalitpur, Nepal

²St. Xavier's College, Maitighar, Kathmandu, Nepal

³Central Department of Physics, Tribhuvan University, Kirtipur, Nepal

⁴Amrit Campus, Tribhuvan University, Kathmandu, Nepal

⁵Sorbonne Universites, LPP, Polytechnique, Paris, France

⁶ T/ICT4D, The Abdus Salam International Center for Theoretical Physics, Trieste, Italy.

*Corresponding author: basudev@sxc.edu.np

Abstract

In this paper, we investigate the performance of the NeQuick 2 (NeQ-2) model with respect to Ciralo's and Gopi's derived ionospheric vertical TEC (vTEC) during the years 2014 and 2015. GPS observables derived from dual-frequency receivers over western Nepal (Simikot, Bhimchula and Nepalganj) are processed to obtain the experimental vTEC utilizing Gopi's and Ciralo's calibration procedures. The monthly and seasonal behavior of vTEC obtained from each calibration technique is compared with the vTEC obtained from the NeQ-2 model during a quiet period. It is observed that the vTEC value obtained from all studied approaches started to increase from 00:00 UT, reached a maximum around 08:00 UT, followed by declination, attaining a minimum value around 23:00 UT. Moreover, a comparative study showed that vTEC computed using the Ciralo calibration technique overestimates GPS vTEC, calculated in all hours and months by Gopi's approach. In the spring and summer, vTEC derived using Ciralo's TEC calibration overestimates NeQ-2 and underestimates it in the autumn and winter. Except for a few day hours in March and April 2014 (solar maximum), NeQ-2 prediction overestimated Gopi calibrated GPS vTEC. In daytime hours, a considerable difference is noted between one vTEC estimate with respect to another. NeQ-2 model vTEC is favourably associated with GPS vTEC obtained using the Gopi procedure in spring and correlates with the Ciralo technique in autumn. Two GPS vTEC estimations demonstrate superior consistency in summer and winter

seasons over all studied stations. The study on geomagnetically disturbed conditions demonstrates that NeQ-2 is not responding to the storm influence. However, the mean absolute difference between NeQ-2 prediction and GPS vTEC procured through the Gopi approach is less on the storm event day. By contrast, it is discovered less by the Ciralo technique when the storm is recovering (except for few cases).

Keywords: Calibration technique, NeQuick model, vTEC, Absolute deviation, Geomagnetic storm

1. Introduction

The ionosphere, an upper atmospheric region comprising free ions and electrons, perturbs the electromagnetic signals passing through it (Appleton, 1932; Hagfors & Schlegel, 2001; Goodman, 2005). The main parameter of the ionosphere responsible for the impedance of trans-ionospheric wave propagation is Total Electron Content (TEC). It is defined as the integrated electron density between the ground receiver and the satellite along one-meter squared ray path through the ionosphere. (Otsuka et al., 2002; Bagiya et al., 2009; Silwal et al., 2021a). TEC is a prime source of error for ground-based receivers to space satellite communication and navigation system (Dabas, 2000; Jin et al., 2007); thus, significant efforts have been made over the last few decades to understand the spatial and temporal variation of ionospheric TEC (e.g. Fejer, 1997; Bhuyan, 2003; Olwendo & Cesaroni, 2016; Ogwala et al., 2019; Silwal et al., 2021b) and to develop TEC models (e.g. Bilitza, 1990; Radicella & Zhang, 1995; Jakowski, 2011; Okoh et al., 2016).

TEC can be estimated using carrier-phase and code observables derived from dual-frequency GNSS receivers (Hernández-Pajares et al., 2011). TEC measured through Dual-frequency GNSS receivers around the Earth is considered the presiding approach for interpreting the ionosphere as they provide data with better accuracy in both time and space (Kumar & Singh, 2011; Fagundes et al., 2016). But TEC derived from carrier-phase measurement is equivocal due to inherent uncertainty in the carrier cycle, whereas estimates using code measurement are typically noisy (Abe et al., 2017). GNSS-TEC data accuracies are limited by instrumental thermal noise, tropospheric effects, higher-order ionospheric effect, and multipath (Mainul & Jakowski, 2012). Thus, GNSS observables should be processed carefully to estimate TEC. A wide range of techniques (Ciralo et al., 2007; Arikan et al., 2004; Montenbruck et al., 2014) has been

developed to realize the accuracy in GNSS-TEC data and every one of them makes distinct presumptions and approximations to simplify the methodology. [Carrano & Groves \(2006\)](#) believes that differential code measurement should be leveled into the differential carrier phase measurement to eliminate the content noise of the code measurements and the undefined ambiguity of the carrier phase. However, some researchers ([Ciraolo et al., 2007](#)) trust that TEC approximation using carrier phase would be enough to avoid the noise content of the code measurement. Whatever the estimation procedure, the dual-frequency GNSS receivers are mighty to compute TEC utilizing the differential delay information they get from different-frequency radio signals.

Despite this, GNSS single frequency systems users rely on ionospheric models to mitigate ionospheric and other navigation errors. Empirical models such as IRI and NeQ-2 are extremely useful since they employ numerical propagation to calculate the electron density at a particular height and the ionospheric TEC ([Rawer et al., 1978](#); [Nava et al., 2008](#)). The NeQ-2 is the evolution of the DGR profiler proposed by [Di Giovanni and Radicella \(1990\)](#). The NeQ-2 profile formulation consists of semi-Epstein layers with a modeled thickness parameter ([Radicella & Leitinger, 2001](#)) and three anchor points: the E-layer peak, the F1 peak, and the F2 peak. These anchor points can be quantified using the ionosonde parameters foE, foF1, foF2, and M (3000) F2 ([Coisson et al., 2006](#)). The NeQ-2 model, which is intended for use in trans-ionospheric propagation applications, has been upgraded on a continuous basis, including NeQuick 1 and NeQuick 2 ([Nava et al., 2008](#)). It is implemented by making considerable improvements to the bottom-side ([Leitinger et al., 2005](#)) and topside ([Coisson et al., 2006](#)) description and optimization of computer programs. This model can estimate TEC up to the height of 20,200 km.

For users of ionospheric models, the accuracy of model prediction is always a primary concern. Comparing ionospheric model estimations to real-time experimental data (from equipment) is a prevalent approach used by ionospheric researchers to assess model accuracy and validate them for useful applications ([Migoya-Orué et al., 2008](#); [Rabiu et al., 2014](#); [Tariku, 2015](#); [Cherniak and Zakharenkova, 2016](#); [Okoh et al., 2018](#); [Sharma et al., 2018](#)). Researchers ([Ezquer et al., 2018](#); [Okoh et al., 2018](#); [Teriku, 2020](#)) conducted a comparison of different ionospheric TEC models (IRI, IRI-plas, and NeQ-2) using GNSS measurements and concluded that NeQ-2 performs better than other models regardless of time or location. [Ahoua et al. \(2018\)](#) compared observed

TEC derived from a nearby GNSS dual-frequency receiver to the NeQ-2 model performance for quiet and storm days over south Africa during the ascending phase of the solar cycle (2009–2011). [Yu et al. \(2012\)](#) evaluated the monthly average of the NeQ-2 model over China during the quietest period and discovered that the NeQ-2 predicts GPS TEC accurately (except for few cases). As indicated previously, there is also considerable variation in the approaches used to estimate the TEC using GNSS observables, and each of them claims to have an accurate approach. Some researchers conducted a comparative study on TEC values derived from various calibration techniques, while others integrated the model with various GPS vTEC estimations ([Abe et al., 2017](#); [Pingelberi et al., 2020](#); [Tornatore et al., 2021](#)). [Abe et al. \(2017\)](#) compared the performance of the calibration approach developed by [Ciraolo et al. \(2007\)](#) (hereafter Ciraolo) and the one developed by [Seemala and Valladares \(2011\)](#) (hereafter Gopi) by using VTEC generated by the European Geostationary Navigation Overlay System Processing Set (EGNOS PS) algorithm as a reference during geomagnetic quiet and disturbance periods. They found that Gopi's approach is more reliable at the low-latitude region and Ciraolo's approach in the mid-latitude region.

As mentioned earlier, several early research studies on the performance of modeled vTEC with respect to GPS vTEC in different solar time and geophysical regions. We have perceived that they have used any TEC calibration techniques to estimate TEC from GPS/GNSS observables and carried out a comparative study to observe model prediction performance to experimental observations. A review of past studies led us to wonder whether model-estimated vTEC performs similarly to vTEC obtained using various GPS TEC estimating approaches. To address this query, we employed the ITU-recommended vTEC model (NeQ-2) in conjunction with two widely used GPS TEC estimating techniques, Gopi's and Ciraolo's. As far as we are aware, no concurrent comparison of the performance of modeled vTEC and GPS vTEC derived using different techniques has been conducted. Also, this is the first study that reports the performance of the NeQ-2 model over the region of Nepal. We believe that this type of study is important not only for determining the model's reliability and validity but also for determining the most appropriate technique for the model's TEC assimilation technique. The paper is organized as follows: Section 2 is for data and methods, and Section 3 is dedicated to results and discussion. The conclusions of all results are summarized in Section 4.

2. Data Set and Methodology

This study used GPS-derived vTEC from Simikot (hereinafter referred to as SMKT), Bhimchula (hereafter referred to as BMCL), and Nepalganj (hereafter referred to as NPGJ) for the years 2014-2015. Table 1 shows the location of stations in geographic and geomagnetic coordinates.

The GPS observables produced by dual-frequency receivers along the studied stations are extracted in the Standard Receiver Independent Exchange (RINEX) format v2.1, a standard ASCII format. UNAVCO makes these data publicly available on its website, <https://www.unavco.org/>. To retrieve the ionospheric observables, the GPS-TEC RINEX files must be processed. The complete explanation of acquiring ionospheric observables using GPS is discussed in [Mannucci et al. \(1999\)](#). For dual-frequency measurement, the path range of signal transmitted from a satellite to the receiver is expressed by carrier phase and Pseudo-range measurement (code measurement) ([Ya'cob et al., 2010](#); [Nie et al., 2018](#)). These measurements are conventionally used to estimate sTEC. The equations to determine sTEC using code and phase measurement are:

$$sTEC_p = \frac{1}{40.3} \left[\frac{1}{L_1^2} - \frac{1}{L_2^2} \right]^{-1} (P_1 - P_2) - (B_s + B_r + e_p) \quad (1)$$

$$sTEC_c = \frac{1}{40.3} \left[\frac{1}{L_1^2} - \frac{1}{L_2^2} \right]^{-1} (\lambda_1 C_1 - \lambda_2 C_2) - (\lambda_1 N_1 + \lambda_2 N_2 + e_c) \quad (2)$$

In the above equations, λ_1 and λ_2 are the wavelengths corresponding to frequency L_1 (1575.42 MHz) and L_2 (1227.60 MHz), respectively. The $sTEC_p$ is the sTEC estimation using code-delay measurement, $sTEC_c$ is the sTEC estimation using carrier phase measurement, P_1 and P_2 are the code-delay measurement on L_1 and L_2 frequency, respectively, B_s indicates the satellite differential code biases, B_r is receiver differential code biases, C_1 and C_2 are the carrier phase measurement on L_1 and L_2 frequency respectively, N_1 and N_2 are the ambiguity integer measure on the carrier phase on L_1 and L_2 frequency respectively, e_p and e_c are the noise and multipath errors concerned with code and carrier phase measurements respectively ([Abe et al., 2017](#)).

As sTEC depends on the elevation of the ray path, equivalent vertical TEC (vTEC) is calculated using the approach proposed by [Klobuchar \(1986\)](#). In this technique, the vTEC is estimated by taking projection from sTEC adopting the thin shell model at the height of around 350 km to 450 km as ionospheric precise point (IPP).

$$vTEC = sTEC \times \cos \left(\sin^{-1} \left[\frac{R_E \cos \Theta}{(R_E + h)} \right] \right) \quad (3)$$

Where R_E is Earth's radius, Θ is the elevation angle at the ground station, and h is the height of precise point (350 km in this study).

Ciraolo's GNSS-TEC calibration is based on carrier-phase measurements from GPS-only or GPS-plus-GLONASS satellite systems without considering code inter-frequency biases (Ciraolo et al., 2007; Abe et al., 2017). On the other hand, Gopi's TEC calibration method takes into account code inter-frequency biases and GPS-only carrier phase measurements. We have used Ciraolo GNSS-TEC (GNSS_2018 version) and Gopi GPS-TEC (GPS Gopi v2.9.4) software. Both TEC estimation software provides $vTEC$ data. We collected data of 15 seconds intervals using GNSS_2018 and 30 seconds using GPS Gopi v2.9.4 TEC calibration software. Later, this observation is converted to an hour resolution by taking the arithmetic mean, resulting in 24 data sets for a given day.

The corresponding modeled $vTEC$ was computed on an hourly basis for a specific day using NeQuick 2. From these hourly data, the mean $vTEC$ for a given month is estimated at a 1-hour resolution. The model package includes FORTRAN 77 subroutines and a driver program. The driver application allows calculating TEC for any ground to satellite ray path. The basic input in the model are coordinates and solar flux and eventually provided $vTEC$ at a specific point in space and time as output. The daily solar flux (F10.7) data made available by the National Oceanic and Atmospheric Administration (NOAA) at <ftp://ftp.swpc.noaa.gov/pub/indices/old/indices/> is utilized as input solar flux for the particular day.

We examined the monthly and seasonal variation in $vTEC$ during quiet days in 2014 and 2015. The years 2014 and 2015 fall within sunspot cycle 24, a relatively short sunspot cycle. The year 2014 occurs during the sunspot cycle's maximum phase, while the year 2015 occurs during the sunspot cycle's declining phase. The top five quiet days of each month were chosen using data from the World Data Center for Geomagnetism in Kyoto (<http://wdc.kugi.kyoto-u.ac.jp/wdc/Sec3.html>). The obtained hourly $vTEC$ measurements of a month's quiet days were processed using simple arithmetic mean to obtain 24 data points for each month of the year under study. Additionally, we chose three geomagnetically disturbed events of varying intensity to

validate the NeQ-2 model's performance during ionospheric disruptions. The Dst, Kp and Ap indexes were used to define the strength and phases of geomagnetic events.

Additionally, seasonal variations were investigated by calculating the arithmetic mean of three months' data for each season: Spring (March, April, and May), Summer (June, July, and August), Autumn (September, October, and November), and Winter (December, January, and February). To compare the different estimations of VTEC and NeQuick2, we present the deviation in vTEC, defined as the difference between the vTEC of the NeQ-2 model (NeQ-2) and the mean vTEC obtained by Ciralo (vTEC (C)) and Gopi (vTEC(G)) approach, at each time each instant of time. Hence,

$$\text{Deviation in vTEC, } d(\text{NeQ-2, Ciralo}) = \text{NeQ-2} - \text{vTEC (C)} \quad (3)$$

$$\text{Deviation in vTEC, } d(\text{NeQ-2, Gopi}) = \text{NeQ-2} - \text{vTEC (G)} \quad (4)$$

This technique has been applied to several previous research works of [Sharma et al. \(2010\)](#), [Amabayo et al. \(2013\)](#), [Silwal et al. \(2021a\)](#).

3. Results and Discussion

In this section, the performance of the real measured data (using Ciralo's and Gopi's TEC calibration techniques) have been evaluated with respect to the model (NeQ-2) observed from the stations: SMKT, BMCL, and NPGJ over the region of Nepal. We primarily discuss the quiet time variation of NeQ-2 prediction regarding Gopi's and Ciralo's TEC calculations and the discrepancy between them through monthly and seasonal analysis. Additionally, we compare one TEC estimation approach to another in a geomagnetically disturbed condition.

3.1 Quiet time monthly variation

Figures 2(a) and 2(b) portray the diurnal variation of the monthly mean vTEC derived utilizing Ciralo's calibration, Gopi's calibration procedures and NeQ-2 model from the stations SMKT, BMCL, and NPGJ of the quiet days of the selected period. It is observed from the figures that vTEC estimated employing all mentioned procedures and model starts increasing from its lowest value around at 00:00 UT (05:45 LT), attain the diurnal maximum peak value at around 08:00 UT (13:45 LT). Hereafter the TEC gradually decreases, attaining a minimum at around 23:00 UT (4:45 LT). This increment in vTEC after sunrise is a very expected phenomenon because the

elevation of solar radiation intensity increases the ionization process in the upper atmosphere causing a high concentration of electrons near the F layer of the ionosphere (Oakh et al., 2018; Sharma et al., 2020). As the sun sets, the reduction of solar radiation amplitude lowers the production of the electron, causing a gradual decrement in TEC. The similar diurnal variation pattern of GPS derived vTEC (both vTEC(C) and vTEC(G)) and NeQ-2 model indicates that NeQ-2 provides a good representation of diurnal TEC variation.

The deviation in mean hourly vTEC from the model and measured using different calibration methods are displayed in Figures 3(a) and 3(b). They demonstrate that the difference in vTEC(C), vTEC(G) and NeQ-2 with respect to one another varies with stations, months and hours of the day. From March to October of 2014 and February to August of 2015, NeQ-2 underestimate vTEC(C) in all hours over all studied regions. However, NeQ-2 overestimate vTEC(C) during the time interval 03:00 -16:00 UT in the remaining months. The maximum difference in vTEC estimation between them is observed between 07:00 - 10:00 UT in March (2014) (< -30 TECU) and 05:00 - 8:00 UT in July (2015) (~ -17 TECU). The low value of deviation between vTEC(C) and NeQ-2 is discerned in August in both years. NeQ-2 overestimate vTEC(G) except in March and few day hours of April, May, and July 2014 (except BMCL). In 2015, the same overestimation was observed except for time intervals 04:00 - 10:00 UT in June and July, 00:00 -8:00 UT in August and morning hours of May. The highest deviation between NeQ-2 and vTEC(G) is observed in the daytime hour of November with 38.49 TECU, 47.66 TECU and 41.88 TECU (10:00 UT in 2014), and 22.19 TECU, 34.07 TECU and 24.57 TECU (09:00 UT in 2015) over SMKT, BMCL and NPGJ stations, respectively. The negligible difference between NeQ-2 and vTEC(G) can be observed after 17:00 UT in October, November, December and January and before 8:00 UT in June and August. The comparative study of two GPS TEC calibrations shows that vTEC(C) overestimate vTEC(G) in all hours and months. It has been found that the largest deviation of vTEC(G) from vTEC(C) occurs during the daytime hour of March (>30 TECU in 2014 and 17 TECU in 2015), while the least deviation has been recorded in August. The overestimation of GPS vTEC derived from the Ciralo's calibration over Gopi calibration technique during the quiet days of October 2013 was shown by Abe et al. (2017) at the grid point of the mid-latitude region.

In addition, the monthly mean vTEC (C) and vTEC(G) was highest in March. However, NeQ-2 showed a maximum mean monthly vTEC in April and November, with an almost similar vTEC count in 2014. On the other hand, we observed significantly low vTEC in November than in April for 2015. This can be due to the impact of solar flux count, which was passed as an input parameter in the NeQ-2 model. NeQ-2 predicts mean electron density from analytical profiles, depending on solar-activity-related input values: sunspot number or solar flux (Nava et al., 2008). High solar radio flux F10.7 in October and November 2014 and significantly low flux count in 2015 can be summarized from figure 5. The lowest mean vTEC is recorded in July 2014 and December 2015 by all vTEC estimation methods over all studied stations.

As a common test framework, our monthly results show that NeQ-2 overestimates or underestimates the GPS- vTEC derived from both approaches at different times and months. Such report is presented in different studies (e.g., Vinkatesh et al., 2014; Chekole et al., 2019: Gopi calibration technique, Olwendo et al., 2016: Ciralo calibration technique). The comparatively low magnitude of monthly mean VTEC is distinguished in 2015 than the year 2014 over all stations. This can be described as the influence of solar activity on the solar cycle. GPS vTEC almost follows the F10.7 index, whose value increases with ascending of the solar cycle and decreases with the fall of the Solar Cycle (Rao et al., 2019). The year 2014 was in solar maxima whereas 2015 in the solar medium, as shown by figure 5. The influence of solar activity on GPS-TEC over the study area is also supported by the report of Guo et al. (2015). Overall analysis shows the semiannual variation in VTEC estimated by either of the approaches.

3.2 Quiet time seasonal variation

This section presented the seasonal trend of NeQ-2, vTEC (C) and vTEC(G) and the discrepancy between them. For this, we have included January and February 2016 to make a full two years' seasonal study (as data of winter months of 2014 were not available).

Figure 3(a) and 3(b) shows that the deviation of vTEC(C) from NeQ-2 is maximum in the spring season. In this season, the deviation is observed in the range of -15.26 - -7.63 TECU in 2014 and between -5.82 and -11.85 TECU in 2015 over studied stations. The lowest deviation was observed in the time interval of 04:00 UT-17:00 UT during winter, where the deviation value is below 5 TECU. In the autumn and winter seasons of studied years, NeQ-2 overestimates vTEC(G) in the time interval of 02:00 UT -16:00 UT but underestimates in other hours of the

day. The NeQ-2 exceeds $vTEC(G)$ for all seasons except few hours in the spring of 2014 and summer of 2015 with nominal value. The highest deviation between them was witnessed at 11:00 UT during autumn with 21.24, 26.90, and 22.86 TECU in 2014 and 19.67, 27.14, 22.26 TECU in 2015 over SMKT, BMCL, and NPGJ, respectively. In spring and summer, deviation plots (fig 6) manifest a low discrepancy between $vTEC(G)$ and NeQ-2. The $vTEC(C)$ overestimates $vTEC(G)$ in all hours and seasons of the studied period. However, the overestimation value is highest during the Spring Season and lowest between the time interval 04:00 - 13:00 UT of the winter.

The mean seasonal $vTEC$ displayed in figure 4 shows the high $vTEC$ count by all studied approaches in spring followed by autumn in 2014, and lowest in Summer. This result supports the report of [Tariku \(2015\)](#). The seasonal variation of $vTEC$ is ascribed to the structure of the magnetic field and the effect of the solar zenith angle ([Rao et al., 2006](#); [Wu et al., 2008](#)). However, [Zou et al. \(2000\)](#) have given credit to change in oxygen and molecular nitrogen concentration in the ionospheric layer as the leading cause of seasonal variations of $vTEC$. In 2015, Ciraolo's and Gopi's calibration estimated the highest mean seasonal $vTEC$ in spring, followed by Summer, Autumn, and Winter. However, NeQ-2 predicted mean seasonal $vTEC$ follows the order: Spring, Autumn, Summer, and winter. Also, NeQ-2 dominates GPS estimations from either of the calibration approaches in autumn, and it overestimates Gopi's calibrated $vTEC$ in all other seasons.

The result from the mean absolute deviation between studied approaches (table 2) shows that the highest mean absolute difference between NeQ-2 and $vTEC(C)$ in the Spring season with a mean absolute deviation of 14.48, 11.10, and 14.57 TECU along with a standard deviation of 2.01, 2.12 and 3.00 (in 2014) and 7.73, 8.77 and 8.75 TECU with a standard deviation 1.77, 1.60, and 1.54 (in 2015) over SMKT, BMCL and NPGJ respectively. On the other hand, in another equinox season, i.e., autumn, a high mean absolute deviation between NeQ-2 and $vTEC(G)$ is observed (see table 2). The high standard deviation between NeQ-2 and $vTEC(G)$ in this season reveals a high discrepancy in deviation value between these approaches. These results manifest the low performance of NeQ-2 with $vTEC(C)$ in the Spring season and with $vTEC(G)$ in the Autumn season. However, in the summer of 2014, NeQ-2 shows good performance with

vTEC(C) but with vTEC(G) in 2015. Similarly, the low mean absolute deviation and standard deviation of vTEC(C) with respect to NeQ-2 in winter of 2014 describe the good performance of NeQ-2 with vTEC(C) in solar maxima. But in the winter of 2015, the standard deviation is higher between NeQ-2 and vTEC(G). The mean absolute deviation between vTEC procured from two calibration approaches is high in spring followed by autumn in 2014, whereas spring followed by Summer in 2015. The lowest mean absolute deviation between them is observed in winter (see table 2).

3.2 Disturb day variation

To study the effect of these three storms on vTEC obtained from mentioned calibration techniques and model, we have considered the mean hourly vTEC value on the storm day, a day before and a day after the storm. The Dst, Kp and Ap indexes were used to define the strength of the storm, which are plotted against Universal time (UT) as shown in the second and third panels of Figures 8, 9, and 10.

As seen in figure 8, the severe storm starts to develop after 7:00 UT on 17 March 2015 with a declination in the Dst index and lasts for around 22:00 UT with a peak Dst index of -223nT. During this period, the peak Kp and Ap value were recorded as 7.7 and 179 nT, respectively. The rapid fluctuation in vTEC (C) and vTEC(G) can be discerned during storm time. However, NeQ-2 responds normally with no significant change in the curve's structure. The gradual decrement in deviation of NeQ-2 from vTEC (C) and between two experimental vTEC is observed with the increment in the storm's intensity. These differences in magnitude are less than the quiet day of March 2015 (refer fig:2 (b)). The recovery phase started and remained throughout the day from the first hour in a universal time on 18th March. On this day, vTEC(G) and vTEC(C) is comparatively lower than the previous day, and no peak was formed during afternoon hours as observed in quiet days of March 2015 (fig:3(b)). Similar findings were also described by [Fagundes et al. \(2016\)](#) over low latitude regions. Nevertheless, NeQ-2 responds normally and overestimates both calibrations, contrasting the result observed on the quiet day of March 2015. The low mean absolute difference and standard deviation value between NeQ-2 and vTEC (G) than vTEC(C) on 17th March 2015 (see table 3) reveals the good performance of NeQ-2 with Gopi's calibration than Ciralo's calibration during the main event day of the storm. However, in the recovery phase, the performance of NeQ-2 is higher with vTEC(C) than

vTEC(G). In comparison to the quiet day of March 2015, the magnitude of mean absolute difference and standard deviation between two calibrations is high in event day (17th March 2015) and low in recovery day (18th March 2015), indicating consistency in the vTEC estimation by two calibration procedures is high in the recovery phase of the severe storm than the main phase.

Figure 9 illustrates the first declination of Dst around 9 UT (-93nT) and again declined to -124 nT at around 22:00 UT on 7th October 2015 with Kp index above 7 and Ap value of 154 nT. It is observed that on 7th October (storm event day), all three approaches have shown similar results except for few mid-day hours. Also, there is an insignificant deviation between vTEC procured from three approaches (except few hours of noontime). This result is different from that observed in the quiet day, where we observed substantial deviation between vTEC(C), vTEC(G), and NeQ-2 (fig 2 (b)). The storm effect on both studied GPS vTEC estimations is observed with oscillation in vTEC value. But as in the previous storm, NeQ-2 does not show a noticeable response to the storm. The low mean absolute difference and standard deviation of NeQ-2 with respect to vTEC(G) than vTEC(C) on 7th October reveal that the performance of NeQ-2 is higher with Gopi's calibration than Ciraolo's (except BMCL, where vTEC(C) shows consistency with NeQ-2) in strong event day (table 3). On 8th October, when the storm goes through the recovery phase, however, the absolute mean deviation of vTEC(G) vs NeQ-2 is low compared to vTEC(C), but the high standard deviation reveals a high discrepancy in the deviation of vTEC(G) from NeQ-2 within the low value. The low absolute mean deviation between two GPS estimations in disturbed days than that of quiet days with low standard deviation reveals a consistency in the estimations of two calibrations in geomagnetic event conditions than in the quiet days.

Figure 10 manifests the variation of vTEC(C) and vTEC(G) and NeQ-2 along with the storm indices during 11-13 September 2015. On 12th September, at around 2:00 UT, Dst declined to -30 UT, revealing a minor storm, but at 16:00 UT, the Dst value increased suddenly from -9 nT to 19 nT and then abruptly decreased to -90 nT at 23:00 UT. At this moment, Kp increased to 6 and Ap around 95 nT. As in the previous storms, a very low discrepancy between vTEC(C), vTEC(G) and NeQ-2 compared to the quiet day of the same month. During the recovery phase, which started after 23:00 UT of 12th September and remained for the whole day of 13th

September, GPS vTEC estimated by both calibrations underestimate NeQ-2. The NeQ-2 did not show a noticeable change in this event as well. The small value of absolute mean difference and small standard deviation between NeQ-2 and vTEC(C) than vTEC(G) on 12th September 2015 manifests more consistency of NeQ-2 with Ciraolo's than Gopi's calibration during moderate storm day. A similar result is obtained on 13th September 2015, which goes through the recovery phase. The consistency in the vTEC estimation by two GPS TEC calibrations is seen in disturbed days than in quiet days. Also, NeQ-2 shows good performance with both calibrations in the main event day but low performance in recovery day in comparison to quiet day (see table 3)

An overall study of NeQuick modeled and GPS vTEC obtained using different calibration approach shows that the NeQuick model does not capture the magnetic storm effects in any of the events, whatever the strength of the storm was, but vTEC (C) and vTEC(G) responds to geomagnetic events by showing rapid fluctuation in vTEC. [Twinomugish et al. \(2017\)](#) also reported a similar result over the east African equatorial region. [Ahoua et al. \(2018\)](#) also concluded that the NeQuick model has comparable reliability in quiet and disturbed days; somewhat, its accuracy is affected by solar activity (better in moderate than in high solar activity). During the storm's main phase, an interplanetary electric field penetrates the ionospheric area for several hours, loading interplanetary particles into the ionosphere ([Kumar and Singh, 2010](#)). This produces a strong decrease in the Dst index during the storm's main phase. The disturbance of the ionospheric region in the main phase could be attributed to the rapid fluctuation of GPS vTEC. Figure (8-10) shows that both GPS-TEC estimation approach responds similarly in a storm event. Our result shows that GPS VTEC estimated by any of the studied approaches experience a decrement in their peak value during the recovery phase compared to event day.

4. Conclusions

In the process of investigating the performance of the TEC model with respect to TEC derived using different GPS- TEC calibration techniques, we have made a comparative study of the NeQ-2 model with two GPS-TEC estimations (Ciraolo's GNSS TEC and Gopi's GPS TEC) using three specific ground-based GPS stations located at the western part of Nepal. The ground-based GPS stations considered in this study lies almost in the same longitude ($81.70 \pm 0.10^\circ$ E) and

near latitude ($29.0 \pm 1.0^\circ$ N) region. We examined the monthly and seasonal quiet time variation vTEC obtained from all three approaches along with the diurnal variation in three geomagnetic events of varying intensity. Based on the results obtained from the study, the following conclusions have been made:

- 1) The GPS vTEC derived using Ciralo's calibration approach overestimates vTEC from Gopi's calibration for all months and all hours over studied stations. In comparison, it overestimates NeQ-2 prediction throughout the spring and summer months while underestimating it during the winter and autumn day hours. Except for a few hours in the spring months of 2014 (March and April), NeQ-2 overestimates Gopi calibrated GPS vTEC.
- 2) In Spring and Autumn, a greater difference between NeQ-2 predicted vTEC and vTEC estimated using the Ciralo calibration process is observed, but a lower deviation is observed in Summer and Winter. However, there is a significant overestimation of NeQ-2 over Gopi-derived vTEC during the autumn and winter months. This demonstrates how NeQ-2 responds differently to various GPS estimation techniques. Furthermore, the difference between the vTEC determined by employing two GPS TEC estimations is highest in the spring months and lowest in the winter months.
- 3) The fact that both GPS-TEC calibration procedures and the NeQ-2 model estimate high TEC values for respective months in 2014 (solar maximum) and low values for respective months in 2015 (solar medium) demonstrates that both GPS and modelled vTEC are affected by solar activity and follow solar parameters such as solar flux F10.7 and sunspot numbers that describe the solar activity.
- 4) The result from the study of mean absolute deviation and standard deviation clearly depicts that NeQ-2 modeled vTEC shows higher performance with vTEC estimated using Gopi approach in Spring season and with Ciralo approached vTEC in Autumn season. In addition, the consistency in the vTEC calculation by two GPS TEC estimation procedure is high in Summer and winter than that of other seasons.
- 5) The lower mean absolute deviation between vTEC estimated by two GPS TEC calibration procedures and the observed lower value of standard deviation in strong and moderate events compared to the quiet days of the respective event months reflects the high performance of two

GPS vTEC estimates compared to each other in a geomagnetically disturbed period than that of a quiet one. However, additional research is necessary to adequately address this finding, which we have placed as future work.

6) NeQ-2 is a climatological model designed to predict the quiet time TEC variation. Our study shows that NeQ-2 model does not capture any of the geomagnetic events. However, we have made a study to figure out the deviation of NeQ-2 prediction in comparison to GPS vTEC estimations under storm effect using two calibration approaches, It is observed that the mean absolute deviation between of Ciralo approached GPS vTEC and NeQ-2 estimation is less in the day when the storm goes through recovery phase whereas deviation between NeQ-2 and GPS vTEC approximated by Gopi procedure is less in main event day (except few cases).

We discovered a disparity in the vTEC values acquired using different processing algorithms, despite the fact that they used the same GPS observable. These discrepancies could be explained by each calibration procedure's bias-leveling computation (Abe et al., 2017). However, the study did not address which method of GNSS-VTEC estimate is the most reliable and appropriate for the analyzed location. In the future, the performance of vTEC estimation utilizing the studied GPS VTEC calibration procedure will be compared to that of alternative calibration techniques and models in order to determine the most effective estimation technique. Furthermore, this study is focused exclusively on the years 2014 and 2015. This work will be expanded in the future to examine the performance of GPS-VTEC and NeQ-2 over prolonged time periods, including solar minimum, when solar activity is low.

Acknowledgements

Solar flux, F10.7 data are obtained from the OMNI (<http://omniweb.gsfc.nasa.gov/>) site. Ground-based dual-frequency GPS TEC data are extracted from the UNAVCO Data Archive (<https://www.unavco.org/>) for the stations mentioned in Table 1. We would like to thank staff members of NASA and UNAVCO for making the data available. In addition, Gopi-derived vTEC is derived from the software GPS Gopi v2.9.4, available at <https://seemala.blogspot.com>. The authors want to thank Gopi Seemala for making the software publicly available for the users. The source code of NeQuick 2 model is provided by the Ionosphere Radiopropagation Unit of the T/ICT4D Laboratory, ICTP under the request of corresponding author.

Author's contribution:

The authors P. Poudel, A. Silwal, S. P. Gautam and M. Karki involved in writing manuscript including data analysis and computations. B. Adhikari, and C. Amory-Mazaudier provided critical feedback with technical details and helped shape the research, analysis and manuscript. D. Pandit contributed to the final version of the manuscript. The work is conducted under the regular guidance of N. P. Chapagain and B. D. Ghimire.

Data availability: All the datasets used for this work can be received upon request to the corresponding author.

Conflict of Interest: The authors declare that they have no conflict of interest.

Funding: This study was conducted under self-funding.

Ethical approval: Not applicable.

References

- Abe, O. E., Villamide, X. O., Papparini, C., Radicella, S. M., Nava, B., & Rodríguez-Bouza, M.: (2017). Performance evaluation of GNSS-TEC estimation techniques at the grid point in middle and low latitudes during different geomagnetic conditions. *Journal of Geodesy* **91**(4), 409-417 (2017). <https://doi.org/10.1007/s00190-016-0972-z>
- Ahoua, S. M., Habarulema, J. B., Obrou, O. K., Cilliers, P. J., & Zaka, Z. K.: Evaluation of the NeQ-2 model performance under different geomagnetic conditions over South Africa during the ascending phase of the solar cycle (2009–2012). *Annales Geophysicae* **36**(5), 1161-1170 (2018). <https://doi.org/10.5194/angeo-36-1161-2018>
- Amabayo EB, Anguma SK, & Jurua E: Tracking the ionospheric response to the solar eclipse of 3 November, 2013. *International Journal of Atmospheric Sciences* vol **2014** Article ID: 127859 (2014). <https://doi.org/10.1155/2014/127859>
- Appleton, E. V.: Wireless studies of the ionosphere. *Institution of Electrical Engineers - Proceedings of the Wireless Section of the Institution* **7**(21), 257–265 (1932). <https://doi.org/10.1049/pws.1932.0027>
- Arikan, F. E. Z. A., Erol, C. B., & Arikan, O.: Regularized estimation of vertical total electron content from GPS data for a desired time period. *Radio Science* **39**(6) (2004). <https://doi.org/10.1029/2004RS003061>
- Bagiya, M. S., Joshi, H. P., Iyer, K. N., Aggarwal, M., Ravindran, S., & Pathan, B. M.: TEC variations during low solar activity period (2005-2007) near the Equatorial Ionospheric Anomaly Crest region in India. *Annales Geophysicae* **27**(3), 1047–1057 (2009). <https://doi.org/10.5194/angeo-27-1047-2009>
- Bhuyan, P. K., Chamua, M., Bhuyan, K., Subrahmanyam, P., & Garg, S. C.: Diurnal, seasonal and latitudinal variation of electron density in the topside F-region of the Indian zone ionosphere at solar minimum and comparison with the IRI. *Journal of atmospheric and solar-terrestrial physics* **65**(3), 359-368 (2003). [https://doi.org/10.1016/S1364-6826\(02\)00294-8](https://doi.org/10.1016/S1364-6826(02)00294-8)
- Bilitza, D.: *International Reference Ionosphere 1990*, National Space Science Data Center, NSSDC 90-22, Greenbelt, Maryland (1990).
- Carrano, C. S., & Groves, K. M.: The GPS segment of the AFRL-SCINDA global network and the challenges of real-time TEC estimation in the equatorial ionosphere. In *Proceedings of the 2006 National Technical Meeting of The Institute of Navigation*, 1036-1047 (2006).

- Chekole, D. A., Giday, N. M., & Nigussie, M.: Performance of NeQuick 2, IRI-Plas 2017 and GIM models over Ethiopia during varying solar activity periods. *Journal of Atmospheric and Solar-Terrestrial Physics* **195**, 105117 (2019). <https://doi.org/10.1016/j.jastp.2019.105117>
- Cherniak, I., & Zakharenkova, I.: NeQuick and IRI-Plas model performance on topside electron content representation: Spaceborne GPS measurements. *Radio Science* **51**(6): 752-766 (2016). <https://doi.org/10.1002/2015RS005905>
- Ciraolo L.: Evaluation of GPS L2-L1 biases and related daily TEC profiles. In *Proceedings of the GPS/ionosphere workshop, Neustrelitz* (pp. 90-97) (1993). <https://doi.org/10.5772/8474>
- Ciraolo, L., Azpilicueta, F., Brunini, C., Meza, A., & Radicella, S. M.: Calibration errors on experimental slant total electron content (TEC) determined with GPS. *Journal of Geodesy* **81**(2), 111–120 (2007). <https://doi.org/10.1007/s00190-006-0093-1>
- Coisson, P., Radicella, S. M., Leitinger, R., & Nava. B.: Topside electron density in IRI and NeQ-2: Features and limitations, *Advances in Space Research* **37**(5), 937–942 (2006). <https://doi.org/10.1016/j.asr.2005.09.015>
- Dabas, R. S.: Ionosphere and its influence on radio communications. *Resonance* **5**(7), 28–43 (2000). <https://doi.org/10.1007/BF02867245>
- Di Giovanni, G., & Radicella, S. M.: An analytical model of the electron density profile in the ionosphere. *Advances in Space Research* **10**(11), 27-30 (1990).
- Ezquer, R. G., Scidá, L. A., Orué, Y. M., Nava, B., Cabrera, M. A., & Brunini, C.: NeQuick 2 and IRI Plas VTEC predictions for low latitude and South American sector. *Advances in Space Research* **61**(7), 1803-1818 (2018). [https://doi.org/10.1016/0273-1177\(90\)90301-F](https://doi.org/10.1016/0273-1177(90)90301-F)
- Fagundes, P. R., Cardoso, F. A., Fejer, B. G., Venkatesh, K., Ribeiro, B. A. G., & Pillat, V. G.: Positive and negative GPS- TEC ionospheric storm effects during the extreme space weather event of March 2015 over the Brazilian sector. *Journal of Geophysical Research: Space Physics* **121**(6), 5613-5625 (2016). <https://doi.org/10.1002/2015JA022214>
- Fejer, B. G.: The electrodynamics of the low-latitude ionosphere: Recent results and future challenges. *Journal of Atmospheric and Solar-Terrestrial Physics*, 59(13), 1465-1482. Jakowski, N., Hoque, M. M., & Mayer, C. (2011). A new global TEC model for estimating transionospheric radio wave propagation errors. *Journal of Geodesy* **85**(12), 965-974 (1997). <https://doi.org/10.1007/s00190-011-0455-1>

Goodman, J. M.: Operational communication systems and relationships to the ionosphere and space weather. *Advances in Space Research* **36**(12), 2241–2252 (2005). <https://doi.org/10.1016/j.asr.2003.05.063>

Guo, J., Li, W., Liu, X., Kong, Q., Zhao, C., & Guo, B.: Temporal-spatial variation of global GPS-derived total electron content, 1999–2013. *PloS one* **10**(7), e0133378 (2015). <https://doi.org/10.1371/journal.pone.0133378>

Hagfors, T., & Schlegel, K.: *Earth's ionosphere. The Century of Space Science, 1559–1584* Springer, Dordrecht (2001). https://doi.org/10.1007/978-94-010-0320-9_64

Hernández-Pajares, M., Juan, J. M., Sanz, J., Aragón-Àngel, À., García-Rigo, A., Salazar, D., & Escudero, M.: The ionosphere: effects, GPS modeling and the benefits for space geodetic techniques. *Journal of Geodesy* **85**(12), 887–907 (2011). <https://doi.org/10.1007/s00190-011-0508-5>

Jakowski, N., Mayer, C., Hoque, M. M., & Wilken, V.: Total electron content models and their use in ionosphere monitoring. *Radio Science* **46**(6) (2011). <https://doi.org/10.1029/2010RS004620>

Jin, S.G., J. Cho, and Park, J.: Ionospheric slab thickness and its seasonal variations observed by GPS. *The Journal of Atmospheric and Solar-Terrestrial Physics* **69** (15), 1864–1870 (2007). <https://doi.org/10.1016/j.jastp.2007.07.008>

Klobuchar, J.: Design and characteristics of the GPS ionospheric time-delay algorithm for single frequency users, in *Proceedings of PLANS'86 – Position Location and Navigation Symposium, Las Vegas, Nevada*, p. 280–286, 4–7 (November 1986).

Kumar, S., & Singh, A. K.: GPS derived ionospheric TEC response to geomagnetic storm on 24 August 2005 at Indian low latitude stations. *Advances in Space Research* **47**(4), 710–717 (2011). <https://doi.org/10.1016/j.asr.2010.10.015>

Kumar, S., & Singh, A. K. (2010, February). The effect of geomagnetic storm on GPS derived total electron content (TEC) at Varanasi, India. In *Journal of Physics: Conference Series* **208**(1), 012062 (2010). <https://doi.org/10.1088/1742-6596/208/1/012062>

Leitinger, R., M.- L. Zhang, and S. M. Radicella: An improved bottomside for the ionospheric electron density model NeQ-2. *Annales of Geophysics* **48**(3), 525–534 (2005).

Mainul, M., & Jakowski, N.: Ionospheric propagation effects on GNSS signals and new correction approaches. *Global Navigation Satellite Systems: Signal. Theory and Applications*, 381–405 (2012). <https://doi.org/10.5772/30090>

Mannucci, A.J.; Iijima, B.; Sparks, L.; Pi, X.Q.; Wilson, B.; Lindqwister, U.: Assessment of global TEC mapping using a threedimensional electron density model. *The Journal of Atmospheric and Solar-Terrestrial Physics* **61**, 1227–1236 (1999). [https://doi.org/10.1016/S1364-6826\(99\)00053-X](https://doi.org/10.1016/S1364-6826(99)00053-X)

Migoya-Oru , Y. M., Radicella, S. M., Coisson, P., Ezquer, R. G., & Nava, B.: Comparing TOPEX TEC measurements with IRI predictions. *Advances in space research* **42**(4), 757-762 (2008). <https://doi.org/10.1016/j.asr.2007.09.041>

Montenbruck, O., Hauschild, A., & Steigenberger, P.: Differential code bias estimation using multi-GNSS observations and global ionosphere maps. In *Proceedings of the 2014 international technical meeting of the Institute of Navigation*, 802-812 (2014).

Nava, B., Coisson, P., & Radicella, S. M.: A new version of the NeQuick ionosphere electron density model. *Journal of Atmospheric and Solar-Terrestrial Physics* **70**(15), 1856-1862 (2008). <https://doi.org/10.1016/j.jastp.2008.01.015>

Nie, W., Xu, T., Rovira-Garcia, A., Zornoza, J. M. J., Subirana, J. S., Gonzalez-Casado, G., ... & Xu, G.: Revisit the calibration errors on experimental slant total electron content (TEC) determined with GPS. *Gps solutions* **22**(3), 1-11 (2018). <https://doi.org/10.1007/s10291-018-0753-7>

Ogwala, A., Somoye, E. O., Ogunmudimu, O., Adeniji-Adele, R. A., Onori, E. O., & Oyedokun, O.: Diurnal, seasonal and solar cycle variation of total electron content and comparison with the IRI-2016 model at Birnin Kebbi. *Annales Geophysicae Discussions*, 1–30 (2019). <https://doi.org/10.5194/angeo-2018-134>

Okoh, D., Onwuneme, S., Seemala, G., Jin, S., Rabi , B., Nava, B., & Uwamahoro, J.: Assessment of the NeQ-2-2 and IRI-Plas 2017 models using global and long-term GNSS measurements. *Journal of Atmospheric and Solar-Terrestrial Physics* **170**, 1-10 (2018). <https://doi.org/10.1016/j.jastp.2018.02.006>

Okoh, D., Owolabi, O., Ekechukwu, C., Folarin, O., Arhiwo, G., Agbo, J., Bolaji, S., Rabi , B.: A regional GNSS-VTEC model over Nigeria using neural networks: A novel approach. *Geodesy & Geodynamics* **7**(1), 19-31 (2016). <https://doi.org/10.1016/j.geog.2016.03.003>

Olwendo, O. J., & Cesaroni, C.: Validation of NeQuick 2 model over the Kenyan region through data ingestion and the model application in ionospheric studies. *Journal of Atmospheric and Solar-Terrestrial Physics* **145**, 143–153 (2016). <https://doi.org/10.1016/j.jastp.2016.04.011>

Olwendo, O. J., Yamazaki, Y., Cilliers, P. J., Baki, P., & Doherty, P.: A study on the variability of ionospheric total electron content over the East African low- latitude region and storm time ionospheric variations. *Radio Science* **51**(9), 1503-1518 (2016). <https://doi.org/10.1002/2015RS005785>

Otsuka, Y., Ogawa, T., Saito, A., Tsugawa, T., Fukao, S., & Miyazaki, S.: A new technique for mapping of total electron content using GPS network in Japan. *Earth, Planets and Space* **54**(1), 63–70 (2002). <https://doi.org/10.1186/BF03352422>

Pignalberi, A., Pietrella, M., Pezzopane, M., & Habarulema, J. B.: Investigating different vTEC calibration methods for data assimilation in ionospheric empirical models. *Advances in Space Research* **68**(5), 2138-2151 (2020). <https://doi.org/10.1016/j.asr.2020.10.040>

Rama-Rao, P. V. S., Gopi Krishna, S., Niranjana, K., & Prasad, D. S. V. V. D.: Temporal and spatial variations in TEC using simultaneous measurements from the Indian GPS network of receivers during the low solar activity period of 2004–2005. In *Annales Geophysicae* **24**(12), 3279-3292 (2006). <https://doi.org/10.5194/angeo-24-3279-2006>

Rabiu, A. B., Adewale, A. O., Abdulrahim, R. B., & Oyeyemi, E. O.: TEC derived from some GPS stations in Nigeria and comparison with the IRI and NeQ-2 models. *Advances in Space Research* **53**(9), 1290-1303 (2014). <https://doi.org/10.1016/j.asr.2014.02.009>

Radicella, S. M., Zhang, M.-L.: The improved DGR analytical model of electron density height profile and total electron content in the ionosphere, *A. Geofisica* **38**, 35-41 (1995). <https://doi.org/10.4401/ag-4130>

Radicella, S.M., Leitinger, R.: The evolution of the DGR approach to model electron density profiles. *Advances in Space Research* **27**(1), 35–40 (2001). [https://doi.org/10.1016/S0273-1177\(00\)00138-1](https://doi.org/10.1016/S0273-1177(00)00138-1)

Rao, S. S., Chakraborty, M., Kumar, S., & Singh, A. K.: Low-latitude ionospheric response from GPS, IRI and TIE-GCM TEC to Solar Cycle 24. *Astrophysics and Space Science* **364**(12), 1-14 (2019). <https://doi.org/10.1007/s10509-019-3701-2>

Rawer, K., Bilitza, D. & Ramakrishnan, S.: Goals and status of the International Reference Ionosphere. *Reviews of Geophysics* **16**(2), 177-181 (1978).
<https://doi.org/10.1029/RG016i002p00177>

Seemala, G. K. & Valladares, C.E.: Statistics of total electron content depletions observed over the South American continent for the year 2008. *Radio Science* **46**(5) (2011).
<https://doi.org/10.1029/2011RS004722>

Sharma, S., Dashora, N., Galav, P. and Pandey R.: Total solar eclipse of July 22, 2009: Its impact on the total electron content and ionospheric electron density in the Indian zone. *Journal of Atmospheric and Solar-Terrestrial Physics* **72**(18), 1387–1392 (2010).
<https://doi.org/10.1016/j.jastp.2010.10.006>

Sharma, S. K., Ansari, K., & Panda, S. K.: Analysis of ionospheric TEC variation over Manama, Bahrain, and comparison with IRI-2012 and IRI-2016 models. *Arabian Journal for Science and Engineering* **43**(7), 3823-3830 (2018). <https://doi.org/10.1007/s13369-018-3128-z>

Sharma, S. K., Singh, A. K., Panda, S. K., & Ansari, K.: GPS derived ionospheric TEC variability with different solar indices over Saudi Arab region. *Acta Astronautica* **174**, 320-333 (2020). <https://doi.org/10.1016/j.actaastro.2020.05.024>

Silwal, A., Gautam, S. P., Chapagain, N. P., Karki, M., Poudel, P., Ghimire, B. D., Mishra R. K. & Adhikari, B.: Ionospheric Response over Nepal during the 26 December 2019 Solar Eclipse. *Journal of Nepal Physical Society* **7**(1), 25-30 (2021b).
<https://doi.org/10.3126/jnphysoc.v7i1.36970>

Silwal, A., Gautam, S. P., Poudel, P., Karki, M., Adhikari, B., Chapagain, N. P., Mishra, R. K., Ghimire, B.D., & Migoya-Orue, Y.: Global positioning system observations of ionospheric total electron content variations during the 15th January 2010 and 21st June 2020 solar eclipse. *Radio Science* **56**(5), 1-20 (2021a). <https://doi.org/10.1029/2020RS007215>

Tariku, Y. A.: TEC prediction performance of the IRI-2012 model over Ethiopia during the rising phase of solar cycle 24 (2009–2011). *Earth, Planets and Space* **67**(1), 1-10 (2015).
<https://doi.org/10.1186/s40623-015-0312-1>

Tariku, Y. A.: Pattern of the variation of the TEC extracted from the GPS, IRI 2016, IRI-Plas 2017 and NeQuick 2 over polar region, Antarctica. *Life sciences in space research* **25**, 18-27 (2020). <https://doi.org/10.1016/j.lssr.2020.02.004>

Tornatore, V., Cesaroni, C., Pezzopane, M., Alizadeh, M. M., & Schuh, H.: Performance Evaluation of VTEC GIMs for Regional Applications during Different Solar Activity Periods, Using RING TEC Values. *Remote Sensing* **13**(8), 1470 (2021). <https://doi.org/10.3390/rs13081470>

Twinomugisha, F., Ssebiyonga, N., & D'ujanga, F. M.: TEC derived from some GPS stations in East African equatorial region and comparison with the TEC from NeQuick2 model. *Advances in Space Research* **60**(9), 1905-1920 (2017). <https://doi.org/10.1016/j.asr.2017.07.018>

Venkatesh, K., Fagundes, P. R., Seemala, G. K., de Jesus, R., de Abreu, A. J., & Pillat, V. G.: On the performance of the IRI- 2012 and NeQuick2 models during the increasing phase of the unusual 24th solar cycle in the Brazilian equatorial and low- latitude sectors. *Journal of Geophysical Research: Space Physics* **119**(6), 5087-5105 (2014). <https://doi.org/10.1002/2014JA019960>

Wu, C. C., Liou, K., Shan, S. J., & Tseng, C. L.: Variation of ionospheric total electron content in Taiwan region of the equatorial anomaly from 1994 to 2003. *Advances in Space Research* **41**(4), 611-616 (2008). <https://doi.org/10.1016/j.asr.2007.06.013>

Ya'acob, N., Abdullah, M., & Ismail, M.: GPS total electron content (TEC) prediction at ionosphere layer over the equatorial region. *Trends in Telecommunications Technologies* (2010). <https://doi.org/10.5772/8474>

Yu, X., She, C., Liu, D., & Zhen, W.: A preliminary study of the NeQuick model over China using GPS TEC and ionosonde data. In *ISAPE2012*, 627-630 (2012). <https://doi.org/10.1109/ISAPE.2012.6408849>

Zou, L., Rishbeth, H., Müller-Wodarg, I. C. F., Aylward, A. D., Millward, G. H., Fuller-Rowell, T. J., & Moffett, R. J.: Annual and semiannual variations in the ionospheric F2-layer. I. Modelling. *Annales Geophysicae* **18**(8), 927- 944 (2000). <https://doi.org/10.1007/s00585-000-0927-8>

Tables captions

Table 1: Details of GPS-stations used in the present study

Table 2: The seasonal mean of absolute deviation of NeQ-2modeled vTEC from GPS vTEC derived using Ciralo calibration technique and Gopi calibration technique, and vTEC deviation between two GPS TEC estimations their standard deviation over SMKT, BMCL, and NPGJ during the quiet days of 2014 and 2015.

Table 3: The mean of absolute deviation of NeQ-2modeled vTEC from GPS vTEC derived using Ciralo calibration technique and Gopi calibration technique, and vTEC deviation between two GPS TEC estimations their standard deviation over SMKT, BMCL, and NPGJ during the event day and the day next to the event.

Figures caption

Figure 1: Map representing the studied station's location. The horizontal axis represents geographical longitude, and the vertical axis represents geographical latitude

Figure 2: Diurnal variation of the monthly averaged GPS VTEC derived from Gopi calibration technique (green curve), Ciruolo calibration technique (red curve), and NeQ- 2 modeled VTEC (blue curve) during the year a) 2014 and b) 2015.

Figure 3: Deviation of monthly averaged diurnal vTEC estimated using Ciruolo and Gopi calibration approach from NeQ-2model vTEC (red and blue bars respectively), vTEC estimated using Gopi calibration approach from Ciruolo calibration approach (green bars) over studied stations for years a)2014 and b) 2015.

Figure 4: Mean monthly vTEC of year obtained using Ciruolo calibration approach, Gopi calibration technique, and NeQ-2 model 2014 and 2015.

Figure 5: Variation of solar flux F10.7 count and Sunspots (R) in solar cycle 24 (2009-2019). The golden shaded region represents the studied period.

Figure 6: Left panel represents the variation of the seasonal averaged diurnal GPS vTEC derived from Gopi calibration technique (green curve), Ciruolo calibration technique (red curve), and NeQ-2modeled vTEC (blue curve), and the right panel represents the deviation of seasonal vTEC estimated using Ciruolo and Gopi calibration approach from NeQ-2modeled vTEC (red and blue bars respectively), vTEC estimated using Gopi calibration approach from Ciruolo calibration approach (green bars) over studied stations for years a)2014 and b) 2015.

Figure 7: Mean seasonal GPS-vTEC obtained using Ciruolo calibration technique, Gopi calibration technique, and NeQ-2 modeled vTEC in 2014 and 2015.

Figure 8: variation of diurnal vTEC estimated using Ciruolo and Gopi calibration approach and NeQ-2modeled vTEC along with the deviation between them during 16-march,2015 to 18 March

2015. The second and third panel of the left side representing the Kp and Ap, and Dst indexes manifests an intense geomagnetic storm on 17 March.

Figure 9: Variation of diurnal vTEC estimated using Ciruolo and Gopi calibration approach and NeQ-2modeled vTEC along with the deviation between them from 6- October 2015 to 8 October 2015. The second and third panel of the left side representing the Kp and Ap, and Dst indexes manifests a strong geomagnetic storm on 7th October.

Figure 10: variation of diurnal vTEC estimated using Ciruolo and Gopi calibration approach and NeQ-2modeled vTEC along with the deviation between them from 11- September 2014 to 13 September 2014. The second and third panel of the left side representing the Kp and Ap, and Dst indexes manifests a moderate geomagnetic storm on 12th September.

Table 1

S.No	Station's Name	Station's location	Geographic Latitude	Geographic Longitude	Geomagnetic Latitude	Geomagnetic Longitude
1	SMKT	Simikot, Nepal	29.9694 ⁰ N	81.8065 ⁰ E	20.99 ⁰ N	156.34 ⁰ E
2	BMCL	Bhimchula, Nepal	28.6558 ⁰ N	81.7144 ⁰ E	19.69 ⁰ N	156.15 ⁰ E
3	NPGJ	Nepalganj, Nepal	28.1172 ⁰ N	81.5953 ⁰ E	19.17 ⁰ N	155.99 ⁰ E

Table 2

Stations	Absolute mean \pm SD for year 2014				Absolute mean \pm SD for year 2015			
	Spring	Summer	Autumn	Winter	Spring	Summer	Autumn	Winter
SMKT								
d(NeQ-2, Ciraolo)	14.48 \pm 2.01	4.13 \pm 1.07	5.26 \pm 3.22	4.39 \pm 2.62	7.73 \pm 1.77	6.91 \pm 2.07	6.54 \pm 3.62	4.43 \pm 2.24
d(NeQ-2, Gopi)	4.22 \pm 2.98	4.06 \pm 2.58	10.59 \pm 6.42	7.39 \pm 4.96	4.62 \pm 1.91	3.46 \pm 1.65	9.68 \pm 6.55	4.08 \pm 3.51
d(Ciraolo, Gopi)	18.10 \pm 1.96	8.18 \pm 2.05	11.70 \pm 1.14	8.51 \pm 1.09	12.35 \pm 0.84	9.03 \pm 1.35	7.38 \pm 0.91	6.04 \pm 1.14
BMCL								
d(NeQ- 2,Ciraolo)	11.10 \pm 2.12	4.32 \pm 0.95	4.89 \pm 3.53	3.96 \pm 3.10	8.77 \pm 1.60	5.89 \pm 1.68	6.57 \pm 3.53	4.52 \pm 2.47
d(NeQ- 2,Gopi)	6.53 \pm 1.95	6.10 \pm 1.77	13.77 \pm 8.61	8.69 \pm 6.17	7.07 \pm 2.64	4.13 \pm 2.16	13.51 \pm 9.96	6.55 \pm 6.22
d(Ciraolo, Gopi)	17.63 \pm 2.12	10.42 \pm 1.50	15.38 \pm 3.09	10.65 \pm 2.61	15.85 \pm 2.59	9.77 \pm 1.17	11.52 \pm 2.96	8.96 \pm 2.06
NPGJ								
d(NeQ-2, Ciraolo)	14.57 \pm 3.00	4.27 \pm 1.03	4.6 \pm 3.56	3.94 \pm 3.27	8.75 \pm 1.54	9.33 \pm 2.87	7.7 \pm 4.45	4.54 \pm 2.78
d(NeQ-2, Gopi)	4.10 \pm 3.01	4.99 \pm 2.19	11.38 \pm 6.89	6.70 \pm 3.96	4.37 \pm 1.86	3.31 \pm 1.54	11.19 \pm 7.83	3.77 \pm 3.15
d(Ciraolo, Gopi)	17.41 \pm 1.79	9.26 \pm 1.66	13.08 \pm 1.89	8.92 \pm 1.37	13.12 \pm 0.66	11.29 \pm 0.64	8.40 \pm 1.22	5.88 \pm 2.16

Table 3

	Severe event		Quiet day	Strong event		Quiet day	Moderate event		Quiet day
	17th March	18th March	March 2015	7th October	8th October	Oct 2015	12th Sept	13th Sept	Sep 2014
SMKT									
d(NeQ-2,Ciraolo)	14.12 ± 7.02	8.32 ± 4.90	7.46 ± 2.63	3.44 ± 1.96	5.03 ± 3.67	6.32 ± 3.58	2.81 ± 2.63	8.17 ± 5.73	4.43 ± 2.79
d(NeQ-2,Gopi)	3.2 ± 2.09	11.0 ± 7.81	7.16 ± 2.49	1.95 ± 1.55	3.93 ± 3.69	9.99 ± 6.90	4.37 ± 2.30	15.03 ± 8.45	7.35 ± 3.70
d(Ciraolo,Gopi)	14.63 ± 6.27	12.92 ± 1.56	14.62 ± 1.57	1.88 ± 1.68	1.54 ± 1.20	7.78 ± 1.29	4.68 ± 3.35	9.13 ± 3.20	11.71 ± 2.98
BMCL									
d(NeQ-2,Ciraolo)	14.28 ± 7.16	8.33 ± 5.13	9.31 ± 3.07	3.82 ± 2.42	5.33 ± 4.23	6.25 ± 3.34	4.74 ± 4.47	7.86 ± 4.74	4.54 ± 3.09
d(NeQ-2,Gopi)	3.89 ± 3.20	13.82 ± 9.88	6.07 ± 2.50	4.15 ± 3.85	5.92 ± 7.54	13.53 ± 9.50	5.29 ± 4.04	17.53 ± 9.92	10.75 ± 5.28
d(Ciraolo,Gopi)	17.16 ± 7.42	14.03 ± 2.45	15.38 ± 3.13	4.45 ± 1.83	5.42 ± 2.49	12.26 ± 3.20	6.57 ± 4.63	13.19 ± 4.00	15.19 ± 3.47
NPGJ									
d(NeQ-2,Ciraolo)	15.81 ± 6.15	8.44 ± 5.46	10.06 ± 3.61	4.08 ± 2.70	5.66 ± 4.41	7.25 ± 3.89	6.26 ± 5.61	7.73 ± 4.42	4.58 ± 2.98
d(NeQ-2,Gopi)	3.35 ± 2.33	10.92 ± 7.42	4.67 ± 2.57	2.80 ± 1.93	4.36 ± 5.47	10.73 ± 7.82	5.47 ± 5.11	15.76 ± 9.38	9.01 ± 4.83
d(Ciraolo,Gopi)	15.4 ± 5.42	9.47 ± 2.49	14.47 ± 2.04	2.52 ± 1.12	2.22 ± 1.11	8.83 ± 1.50	6.60 ± 4.24	12.14 ± 4.54	13.55 ± 3.71

Figure 1

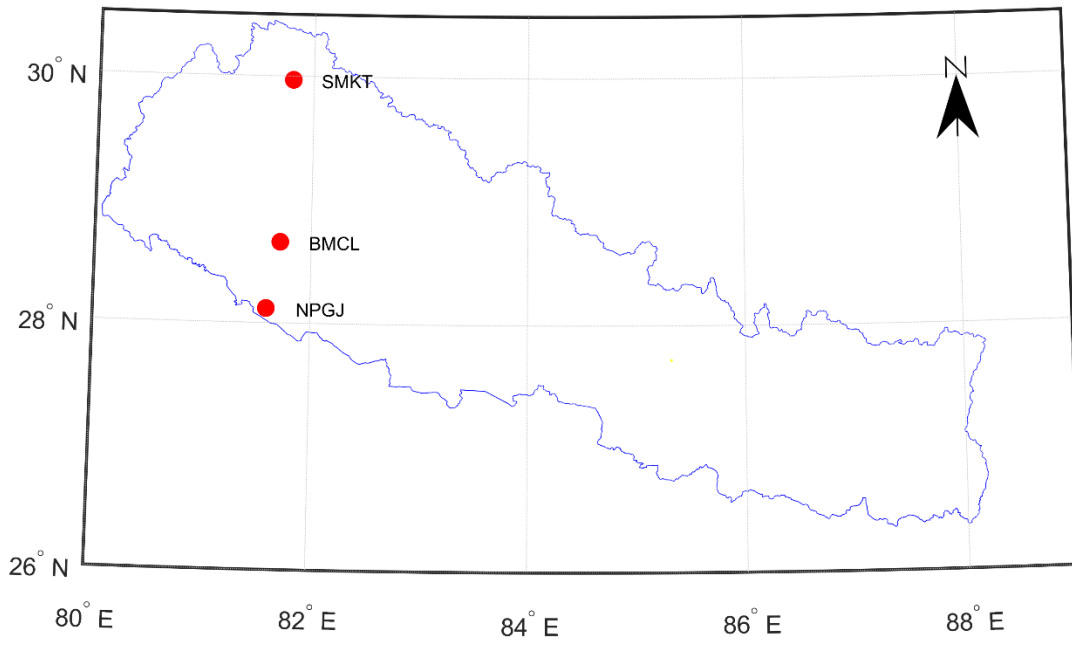


Figure 2

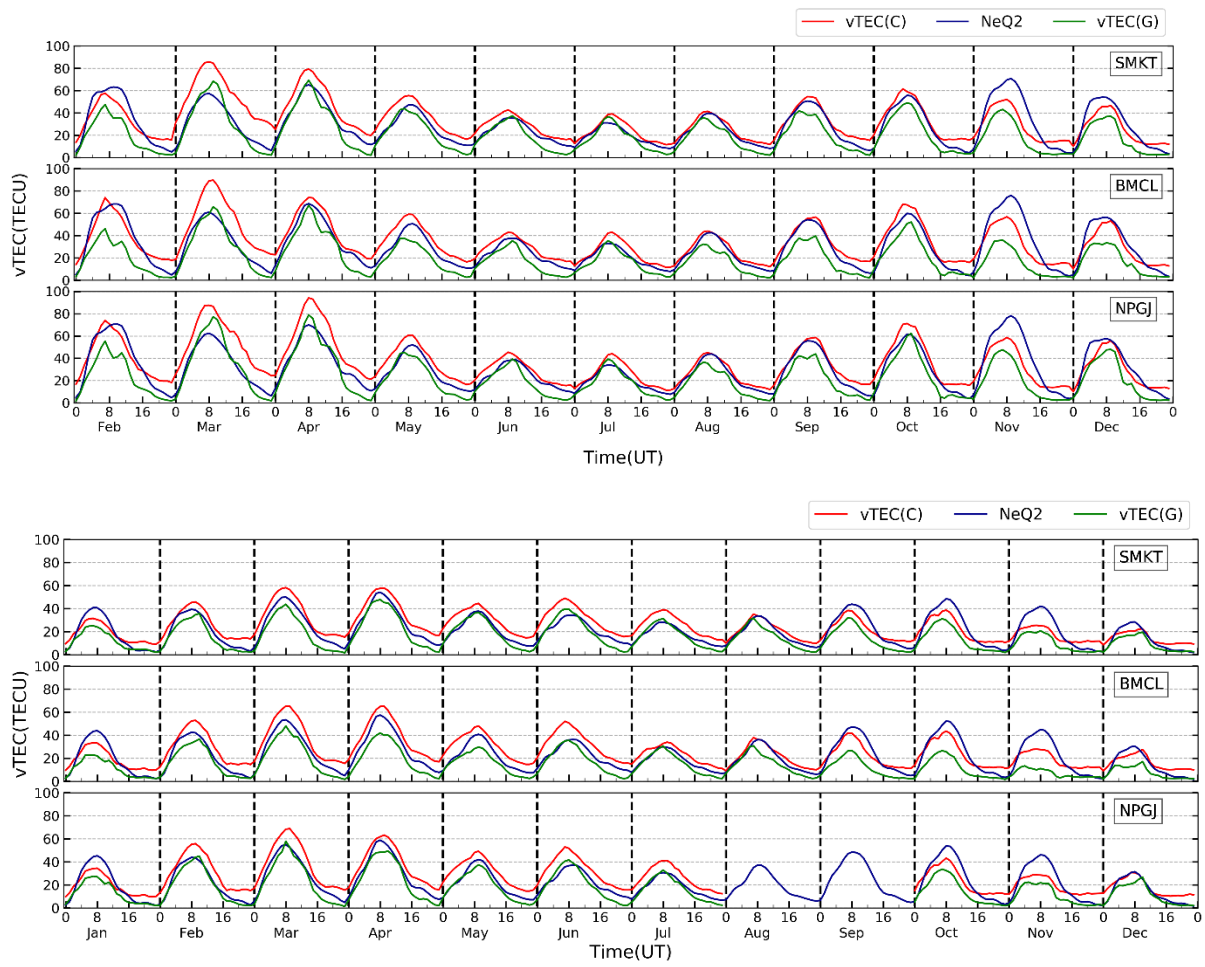


Figure 3

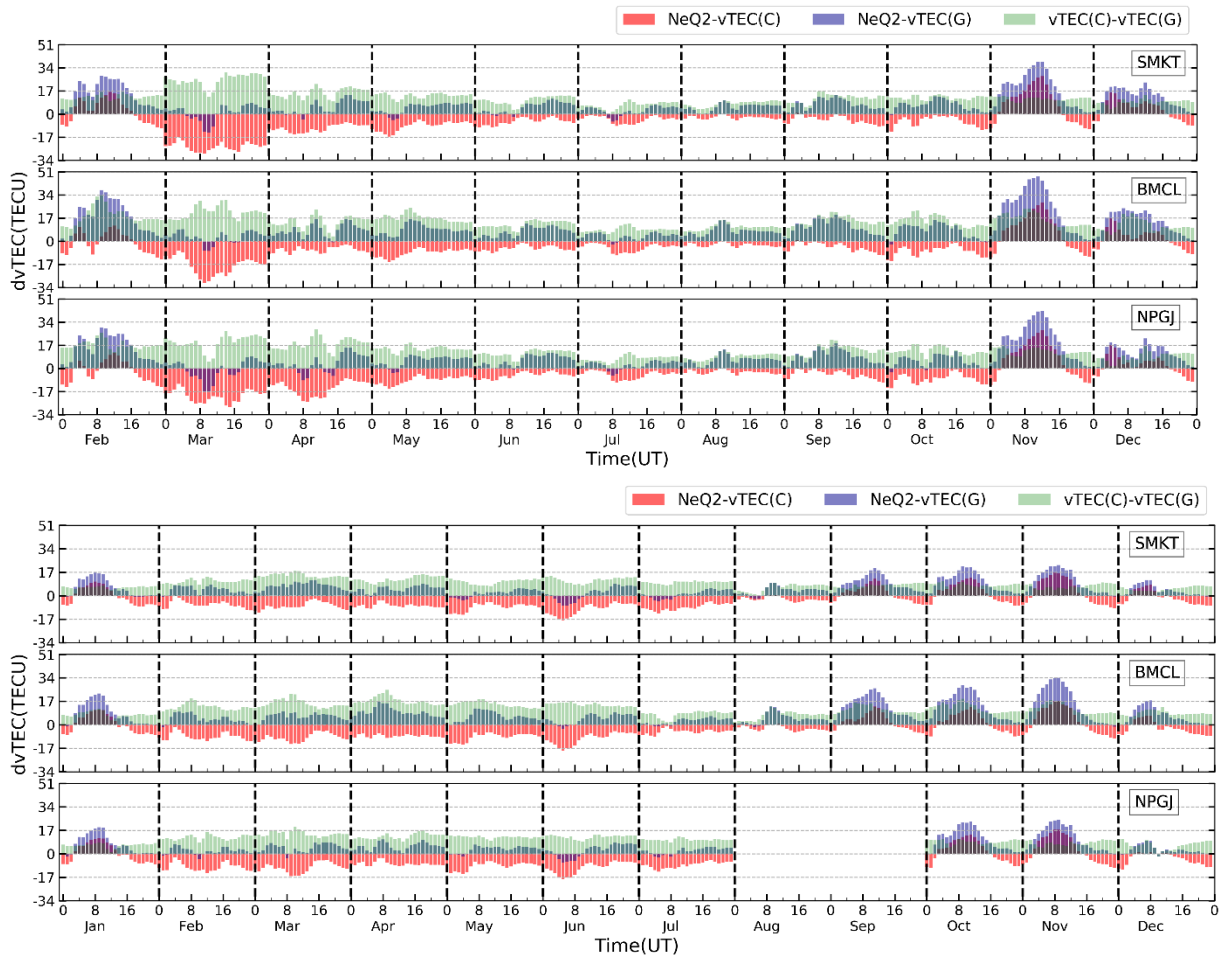


Figure 4

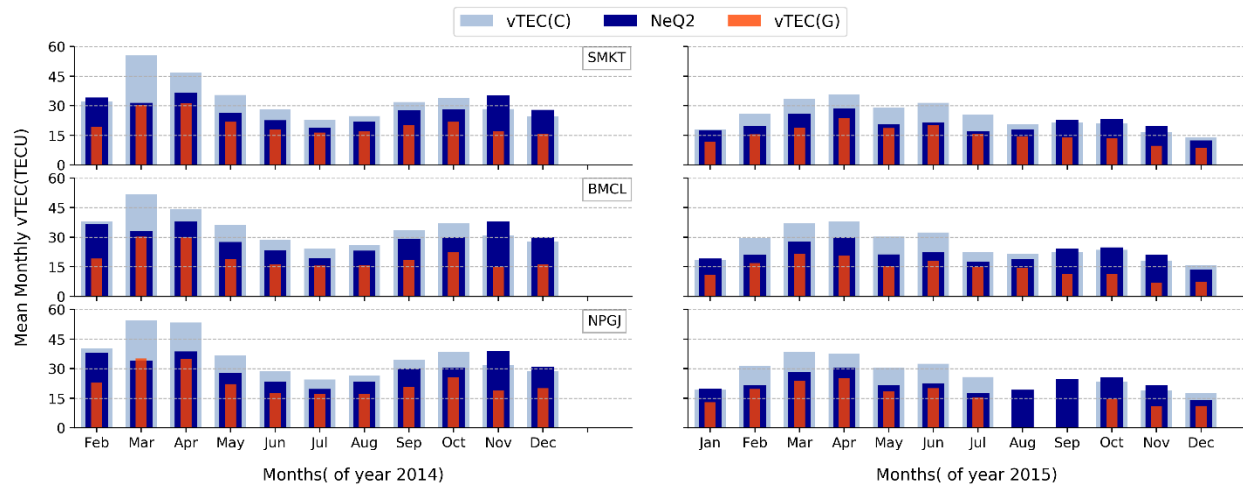


Figure 5

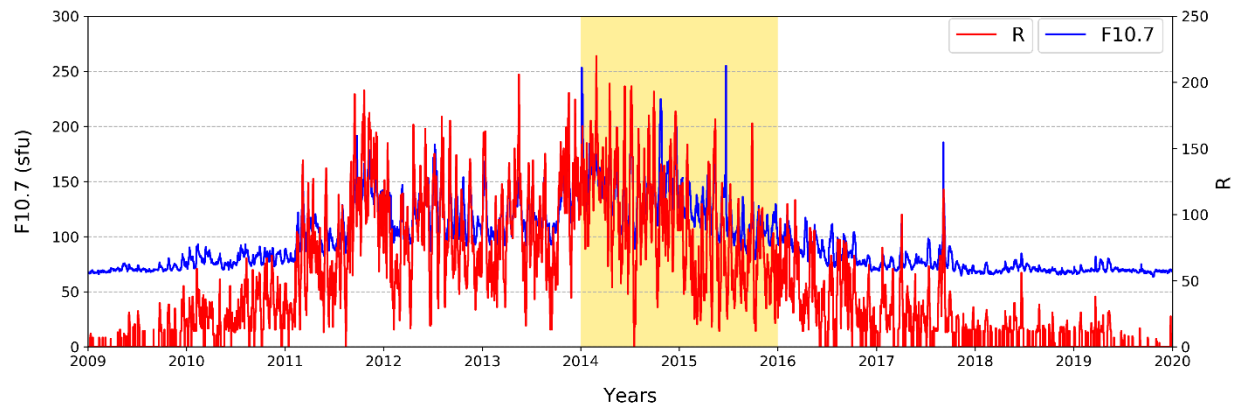


Figure 6

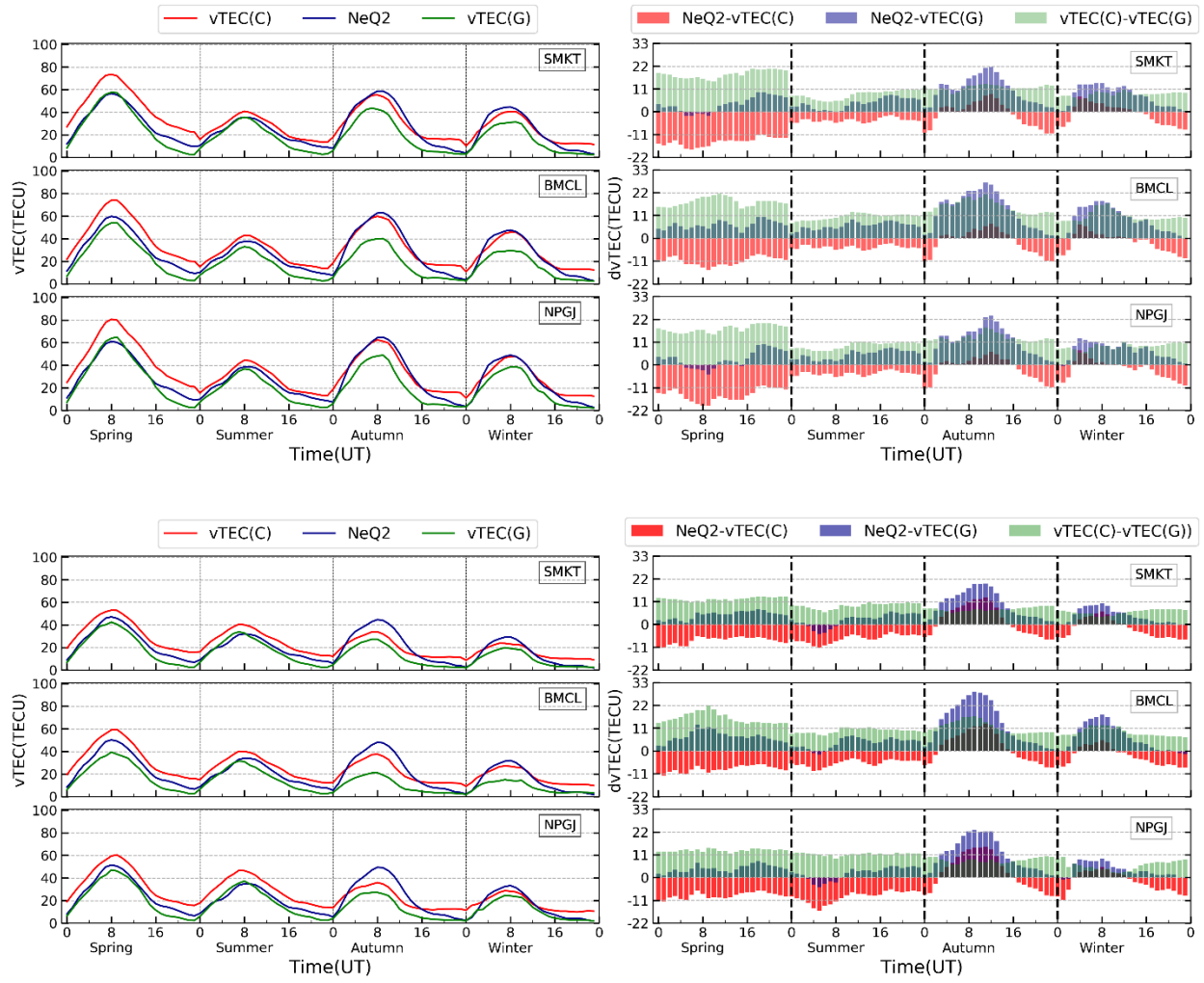


Figure 7

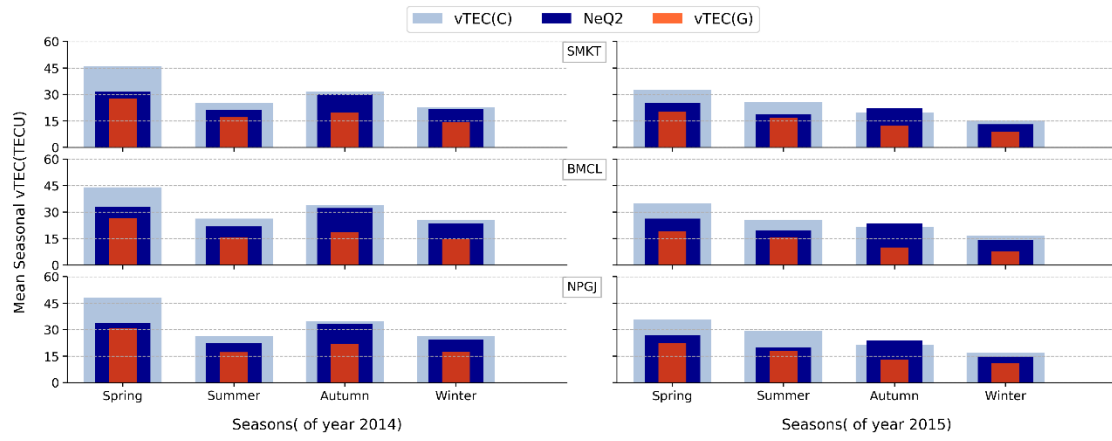


Figure 8

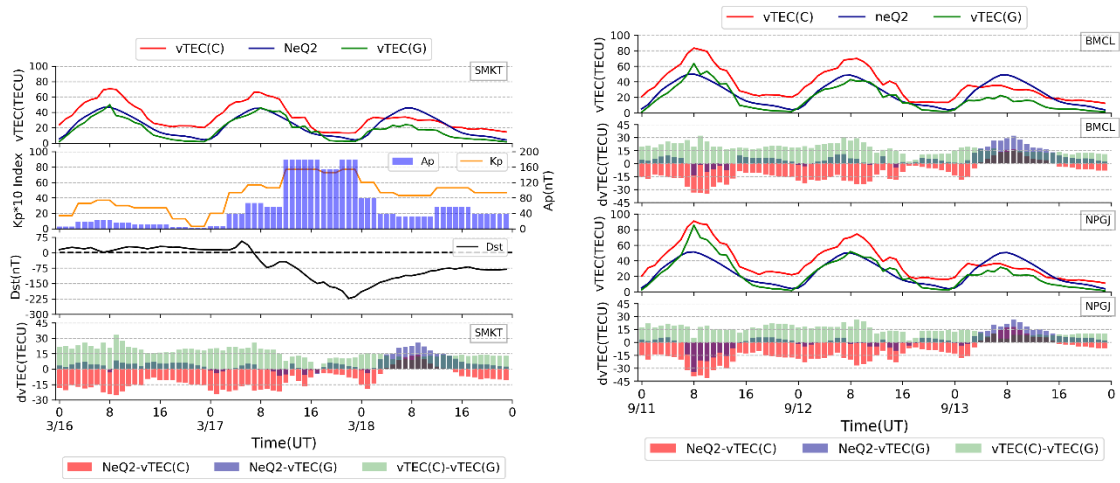


Figure 9

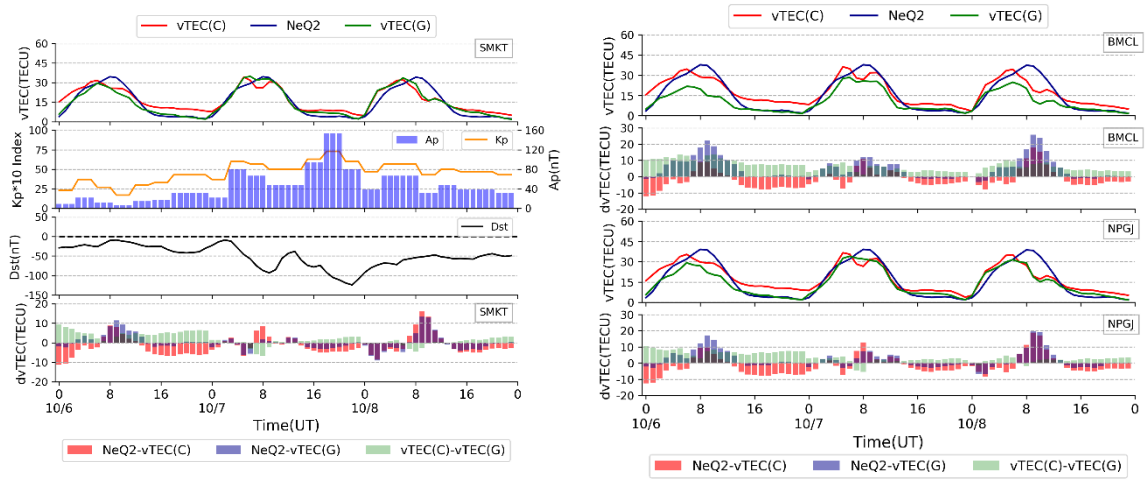


Figure 10

